

Combustion for aerospace propulsion

Eulerian models for turbulent spray combustion with polydispersity and droplet crossing

S. de Chaisemartin ^a, L. Fréret ^a, D. Kah ^{a,b}, F. Laurent ^{a,*}, R.O. Fox ^c, J. Reveillon ^d,
M. Massot ^a

^a Laboratoire EM2C-UPR CNRS 288, École centrale Paris, grande voie des vignes, 92295 Chatenay-Malabry cedex, France

^b Institut français du pétrole, 1&4, avenue de Bois-Préau, 92852 Rueil-Malmaison cedex, France

^c Department of Chemical and Biological Engineering, 2114 Sweeney Hall, Iowa State University, Ames, IA 50011-2230, USA

^d CORIA – UMR CNRS 6614, université de Rouen, avenue de l'université, B.P. 12, 76801 Saint-Etienne-du-Rouvray, France

Available online 21 July 2009

Abstract

The accurate simulation of the dynamics of polydisperse evaporating sprays in unsteady gaseous flows with large scale vortical structures is both a crucial issue for industrial applications and a challenge for modeling and scientific computing. The difficulties encountered by the usual Lagrangian approaches make the use of Eulerian models attractive, aiming at a lower cost and an easier coupling with the carrier gaseous phase. Among these models, the multi-fluid model allows the detailed description of polydispersity and size/velocity correlations for droplets of various sizes. The purpose of the present study is two-fold. First, we extend the multi-fluid model in order to cope with droplet trajectory crossings by using the quadrature method of moments in velocity phase space conditioned by size. We identify the numerical difficulties and provide dedicated numerical schemes in order to preserve the velocity moment space. Second, we conduct a comparison study and demonstrate the capability of such an approach to capture the dynamics of an evaporating polydisperse spray in a two-dimensional free jet configuration. We evaluate the accuracy and computational cost of Eulerian models and related discretization schemes versus Lagrangian solvers. It shows that, even for finite Stokes number, the standard Eulerian multi-fluid model is accurate at reasonable cost. *To cite this article: S. de Chaisemartin et al., C. R. Mecanique 337 (2009).*

© 2009 Published by Elsevier Masson SAS on behalf of Académie des sciences.

Résumé

Modèles eulériens pour la combustion turbulente de spray polydispersés avec croisement de gouttes. La simulation prédictive de la dispersion turbulente de spray évaporant polydispersés est à la fois un enjeu crucial pour les applications industrielles et un défi majeur pour la modélisation et le calcul scientifique. Les difficultés rencontrées par les approches lagrangiennes habituellement utilisées rendent l'alternative proposée par les méthodes eulérienne attractive, afin d'obtenir un coût de calcul plus faible et un couplage avec la description de la phase gazeuse simplifiée. Parmi les modèles eulériens, le multi-fluide permet de décrire précisément la polydispersion et les corrélations taille/vitesse pour toute la gamme de tailles de gouttes. L'objectif de cette étude est double. Tout d'abord le multi-fluide est étendu afin de décrire les croisements de trajectoires en utilisant une méthode de quadrature de moments conditionnée par la taille pour l'espace des phases en vitesses. Les difficultés numériques sont identifiées et un schéma numérique dédié, permettant de préserver l'espace des moments, est construit. Ensuite une étude comparative nous permet de démontrer la capacité d'une telle approche pour prédire la dynamique d'un brouillard de gouttes polydispersé en évaporation

* Corresponding author.

E-mail address: frederique.laurent@em2c.ecp.fr (F. Laurent).

dans un jet libre bi-dimensionnel. La précision de la méthode ainsi que son coût de calcul sont évalués par comparaison à des résultats de solveurs lagrangiens. Cette étude nous permet de montrer l'efficacité, pour un coût de calcul raisonnable de la méthode eulérienne multi-fluide. *Pour citer cet article* : S. de Chaisemartin et al., *C. R. Mécanique* 337 (2009).

© 2009 Published by Elsevier Masson SAS on behalf of Académie des sciences.

Keywords: Fluid mechanics; Two-phase flow; Combustion; Numerical simulation; Eulerian methods; Moment method

Mots-clés : Mécanique des fluides ; Ecoulement diphasique ; Combustion ; Simulation numérique ; Méthodes eulériennes ; Méthodes de moments

1. Introduction

Many industrial devices involve turbulent combustion of an evaporating liquid phase. In the transport sector, rocket, aircraft or car engines are almost exclusively based on storage and injection of a liquid fuel, which is sprayed into a chamber where turbulent combustion takes place. It is of primary importance to understand and control the physical processes as a whole from the injection into the chamber up to the combustion phenomena.

Numerical simulation is now a standard tool to optimize turbulent combustion processes in such devices. If purely gaseous problems are well known with a wide range of suggested closures, it is not the case for two-phase flows with combustion where one needs detailed turbulent combustion of two-phase flows, one needs information about the physics of the triple interactions: spray/turbulence/combustion.

Generally speaking, two approaches for treating liquid sprays corresponding to two levels of description can be distinguished. The first, associated with a full direct numerical simulation (DNS) of the process, provides a model for the dynamics of the interface between the gas and liquid, as well as the exchanges of heat and mass between the two phases using various techniques such as the Volume of Fluids or Level Set methods. The second approach, based on a more global point of view, describes the droplets as a cloud of point particles, the geometry of which are presumed spherical, and for which the exchange of mass, momentum and heat are described globally. It is the only one for which numerical simulations at the scale of a combustion chamber or in a free jet can be conducted. Thus, this “mesoscopic” point of view will be adopted in the present study.

In the mesoscopic framework, there exists considerable interest in the development of numerical methods for simulating sprays relying on a transport equation given by [1], based on kinetic theory. The principal physical processes that must be accounted for are: (1) transport in physical space; (2) evaporation; (3) acceleration of droplets due to drag; and (4) break-up, rebound and coalescence leading to polydispersity. The major challenge in numerical simulations is to account for the strong coupling between these processes. In the context of one-way coupling, the Lagrangian Monte-Carlo approach, called Direct Simulation Monte-Carlo method (DSMC) by [2], is generally considered to be more accurate than Eulerian methods for solving Williams equation. However, its computational cost is high, especially in unsteady configurations. Moreover, in applications with two-way coupling, Lagrangian methods are difficult to couple accurately with Eulerian descriptions of the gas phase. There is thus considerable impetus to develop Eulerian methods, keeping in mind that such models still need validation through comparisons with the Lagrangian approach and experimental measurements.

However, there exists two shortcomings of the actual Eulerian models. First, they fail to describe polydispersity; however, in many industrial configurations evaporating droplets of different sizes follow different pathways thus depositing their fuel mass fraction at different places. One way to solve the problem is to use multi-fluid models [3]. Second, Eulerian models are derived from Williams equations through an equilibrium assumption leading to closure at the level of velocity moment equations conditioned by droplet size. The model is not able to capture multi-modal droplet velocity distribution and thus droplet crossing, but is essentially monokinetic. Even if the multi-fluid model can afford droplet crossing for droplets of different sizes, the equilibrium assumption is too limiting and leads to the creation of singularities, which have been studied analytically in [3] with a physical interpretation in [4]. Recently, the use of the quadrature method of moments in the velocity phase space has provided a closure for non-equilibrium velocity distributions for monodisperse particles allowing to capture droplet crossing at finite Stokes number with the use of Eulerian model [5].

The present study provides a new Eulerian model, as well as dedicated numerical schemes, able to deal with polydispersity as well as non-equilibrium velocity distributions for evaporating sprays. The proposed method satisfies a crucial property: the preservation of the moment space. The model is validated in a free jet configuration by detailed

comparison with a Euler–Lagrange solver provided by [6]. After showing the accuracy of the model at capturing the dynamics of droplets of various sizes, we investigate its ability to properly evaluate the gaseous fuel mass fraction field issuing from evaporation. The final objective is the evaluation of the relative accuracy and computational cost between Eulerian and Lagrangian approaches. The framework of the study is DNS. However, in the context of LES, Eulerian model will encounter the same issues from both a modeling and computational point of view.

2. Statistical description at the mesoscopic scale and Lagrangian discretization

At the mesoscopic scale, droplets are described as a cloud of point particles for which the exchange of mass, momentum and heat are described globally, using eventually correlations, and the details of the interface behavior, angular momentum of droplets, etc., are not predicted. For the gaseous phase, L_0 denotes a reference length, U_0 a reference velocity and $t_0 = L_0/U_0$ the associated time scale, and a typical kinematic viscosity ν_0 allows to define a Reynolds number. For the spray, S_0 denotes a reference droplet surface, $t_{p0} = \rho_{l0}S_0/(\rho_{g0}18\pi\nu_0)$ is the droplet dynamical time that defines the Stokes number $St = t_{p0}/t_0$, where ρ_{l0} and ρ_{g0} are references liquid and gas densities respectively. In the following, even if heating can easily be included in the models, we will restrict the framework of the study to evaporation and drag. In the present study, we make the assumption that these quantities only depend on the local gaseous phase as well as on the state of the k th droplet. In addition, we suppose that all the scales of the gaseous phase are resolved in the context of DNS. We adopt a statistical description of the Boltzmann type and the spray can be described by its joint surface, velocity non-dimensional number density function (NDF) $f(t, \mathbf{x}, S, \mathbf{u})$, which satisfies the transport equation of [1]:

$$\partial_t f + \partial_{\mathbf{x}} \cdot (\mathbf{u}f) + \partial_S(Kf) + \partial_{\mathbf{u}} \cdot (\mathbf{F}f) = \frac{1}{Kn} \Gamma$$

where, for the sake of simplicity of our investigation, K is the constant of a d^2 law and $\mathbf{F} = (\mathbf{U}_g(t, \mathbf{x}) - \mathbf{u})/(St S)$ is a linear drag force per unit mass, \mathbf{U}_g is the gas non-dimensional velocity and all the involved quantities are non-dimensional. The collision operator Γ , will not be taken into account in this contribution but is described in [7]. The Knudsen number Kn , is the ratio between the mean free path $l_0 = 1/(n_0\sigma_0)$ and L_0 , where σ_0 is the typical collision cross section and n_0 a typical droplet number density. In the limit of small particles and dilute sprays, the Knudsen number is large enough so that the effect of the collision operator becomes negligible.

In this context, the Williams equation can be discretized through a Particle Discretization (PD), where the NDF is represented by a sum of Dirac delta functions:

$$f(t, \mathbf{x}, \mathbf{u}, S) = \sum_p w_p \delta(\mathbf{x} - \mathbf{x}_p(t)) \delta(\mathbf{u} - \mathbf{u}_p(t)) \delta(S - S_p(t))$$

where w_p is a constant weight of the k th numerical particle and \mathbf{x}_p , \mathbf{u}_p , S_p are its position, velocity and surface, respectively. These characteristics of numerical particles evolve through standard differential equations involving drag acceleration \mathbf{F} and evaporation rate K . This method provides, if enough numerical particles are used, an ensemble average of the droplet repartition and then can yield Eulerian fields. Under the particular set of assumptions we have chosen, it is equivalent to an ensemble of discrete particle simulations (DPS) where each individual numerical particle represents one droplet and the weights are equal to one such as what is done in [6]. The number density of particles for DPS is then evaluated with respect to a given equivalence ratio for evaporation and combustion purposes and it corresponds to one realization of an ensemble average governed by the Williams equation.

3. Development of the Eulerian multi-fluid multi-velocity approach

3.1. Standard Eulerian multi-fluid model and its limitations

The formalism and the associated assumptions needed to derive the Eulerian multi-fluid model were originally introduced in [8] extending the ideas of [9]. We recall briefly the main features:

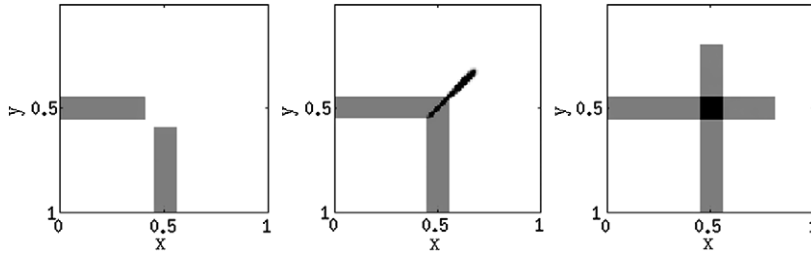


Fig. 1. Simulation of crossing jets before collisions at time $t = 0.4$ (left) and after collision at time $t = 0.8$ using the multi-fluid model (center) and the multi-fluid multi-velocity model (right).

[H1] We presume the form of the NDF $f(t, \mathbf{x}, S, \mathbf{u}) = n(t, \mathbf{x}, S)\delta(\mathbf{u} - \bar{\mathbf{u}}(t, \mathbf{x}, S))$ through a single node quadrature method of moments in velocity phase space conditioned by size, where $\bar{\mathbf{u}}(t, \mathbf{x}, S)$ is the average velocity conditioned by droplet size.¹

[H2] The droplet size phase space is divided into intervals $[S_{k-1}, S_k[$, called sections. In one section, $\bar{\mathbf{u}}^{(k)}$ does not depend on droplet size. The form of $n^{(k)}(t, \mathbf{x}, S) = m^{(k)}(t, \mathbf{x})\kappa^{(k)}(S)$ as a function of S is assumed independent of (t, \mathbf{x}) in each section, and the variable used is $m^{(k)} = \int_{S_{k-1}}^{S_k} \rho_l S^{3/2} n^{(k)} dS$, the non-dimensional mass density in section k relative to the typical mass density, $m_0 = \rho_{l0} S_0^{3/2} n_0 / (6\sqrt{\pi})$.

The set of droplets in one section can be seen as a “fluid” for which conservation equations are written, thus yielding exchanges of mass and momentum between the coupled fluids. Droplets in different sections can then have different dynamics with an a priori control of the precision required in the size phase space. Let us note that such an approach only focuses on one moment of the distribution in the size variable within each section, and the mass moment is chosen because of its relevance in the evaporation and combustion process. Higher order approximations can be used (see [10] and references therein).

The conservation equations for the k th section then read:

$$\left. \begin{aligned} \partial_t m^{(k)} + \partial_{\mathbf{x}} \cdot (m^{(k)} \bar{\mathbf{u}}^{(k)}) &= (E_1^{(k)} + E_2^{(k)})m^{(k)} - E_1^{(k+1)}m^{(k+1)} \\ \partial_t (m^{(k)} \bar{\mathbf{u}}^{(k)}) + \partial_{\mathbf{x}} \cdot (m^{(k)} \bar{\mathbf{u}}^{(k)} \otimes \bar{\mathbf{u}}^{(k)}) &= (E_1^{(k)} + E_2^{(k)})m^{(k)} \bar{\mathbf{u}}^{(k)} - E_1^{(k+1)}m^{(k+1)} \bar{\mathbf{u}}^{(k+1)} + m^{(k)} \bar{\mathbf{F}}^{(k)} \end{aligned} \right\} \quad (1)$$

where $E_1^{(k)}$ and $E_2^{(k)}$ are the evaporation coefficients and $\bar{\mathbf{F}}^{(k)}$ is the averaged drag force, function of a mean surface of the section $S_{\text{mean}}^{(k)}$. The $E_1^{(k)}$ and $E_2^{(k)}$ terms represent the exchange between successive sections and exchange with the gaseous phase through evaporation, respectively. These conservation equations have the same mathematical structure as the pressure-less gas dynamics equation. They potentially lead to singular behavior and require well-suited numerical methods (see [3,4]).

One typical configuration for which the Eulerian multi-fluid model predicts an artificial averaging is when two droplet jets are crossing for a monodisperse spray. Indeed, at the collision location, there exist at the same space and time location two velocities leading to a bi-modal velocity distribution that is out of equilibrium. This configuration is presented in Fig. 1 without drag nor evaporation, or in a more complex case with drag and evaporation in Fig. 2. The Eulerian multi-fluid multi-velocity model, presented in the next subsection, predicts in Fig. 1-right the exact solution (CFL number is always one) for this simple configuration for which the two jets do not interact in the chosen “infinite Knudsen limit”. In Fig. 2-right the multi-fluid multi-velocity model can describe the crossing of the jets, nevertheless, due to evaporation and drag, the CFL number is no longer unitary. The classical multi-fluid method, because of the equilibrium assumption [H1], cannot handle this case. Only different size droplets can experience crossing within this framework. Thus we switch to an artificial collisional “zero Knudsen limit” presented in Figs. 1-center and 2-left where a δ -shock is created.

¹ This corresponds to a generalized Maxwell–Boltzmann distribution at zero temperature and remains an “equilibrium” velocity distribution even if there is no collision operator in the model.

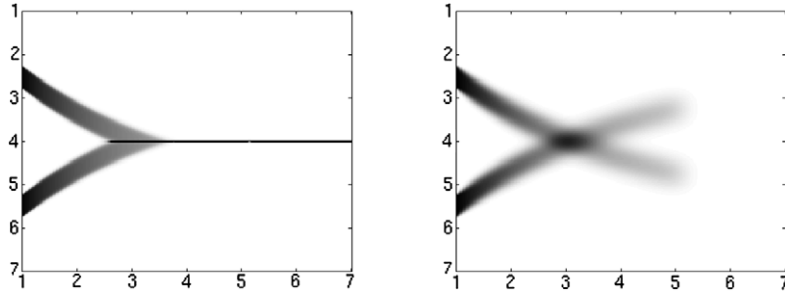


Fig. 2. Simulation of crossing jets with drag and evaporation at time $t = 10$ using the multi-fluid model (left) and the multi-fluid multi-velocity model (right).

3.2. Multi-velocity approach

Assumption [H1] corresponds to a one-node quadrature based on the moments of order lower or equal to one in velocity. Since it is too restrictive, within the k th section, we extend [H1] and assume the following form for the NDF:

$$f(t, \mathbf{x}, S, \mathbf{u}) = n^{(k)}(t, \mathbf{x}, S)g^{(k)}(t, \mathbf{x}, \mathbf{u})$$

where n is the size number density function that still satisfies [H2], and g the velocity probability density function, which is assumed independent of size variations inside the k th section. We consider the same mass-velocity moments of the NDF defined for the k th section by

$$m^{(k)} M_{j,l}^{(k)} = \int_{S_{k-1}}^{S_k} \rho_l S^{3/2} n^{(k)} dS \int_{\mathbf{u}} (u_x)^j (u_y)^l g^{(k)}(t, \mathbf{x}, \mathbf{u}) d\mathbf{u}$$

relying on the moments up to order 3, and the moment transport equation system reads, from Eq. (1), with $j + l \leq 3$:

$$\begin{aligned} \partial_t m^{(k)} M_{j,l}^{(k)} + \partial_x (m^{(k)} M_{j+1,l}^{(k)}) = & -(E_1^{(k)} + E_2^{(k)}) m^{(k)} M_{j,l}^{(k)} + E_1^{(k+1)} m^{(k+1)} M_{j,l}^{(k+1)} \\ & + j m^{(k)} \frac{U_{g,x} M_{j-1,l}^{(k)} - M_{j,l}^{(k)}}{\text{St} S_{\text{mean}}^{(k)}} + l m^{(k)} \frac{U_{g,y} M_{j,l-1}^{(k)} - M_{j,l}^{(k)}}{\text{St} S_{\text{mean}}^{(k)}} \end{aligned} \quad (2)$$

In order to close the transport in physical space, and to be able to extend this method to more complex models, we will use a quadrature method of moments in the spirit of [5]. Let $d = 2$ denote the number of velocity phase space dimensions and $\alpha \in 1, \dots, 2^d$ denote the set of weights and abscissas for the $2^d = 4$ -node quadrature approximation of g . The velocity moments are easily related to the quadrature weights $\omega_\alpha^{(k)}$ and abscissas $(u_{\alpha,x}^{(k)}, u_{\alpha,y}^{(k)})$ by $M_{j,l}^{(k)} = \sum_{\alpha=1}^{2^d} \omega_\alpha^{(k)} (u_{\alpha,x}^{(k)})^j (u_{\alpha,y}^{(k)})^l$, where $j + l \leq 3$, whereas the issue is to evaluate the abscissas and weights from the data of the velocity moment vector of size 10. The correspondence is one-to-one in one space dimension. However, in dimension greater or equal to two, we will transport the whole set of moments but effectively restrict the moment subspace recursively structured from the set of second-order velocity moments for which the correspondence is one-to-one, and insure that the velocity moment vector lives in this subspace.

We introduce a linear transformation $\mathbf{L}^{(k)}$ as well as a rotation matrix, such that

$$(R^{(k)} \mathbf{L}^{(k)})^T R^{(k)} \mathbf{L}^{(k)} = (\sigma_{ij}^{(k)})_{i \in \{x,y\}, j \in \{x,y\}} = \sigma^{(k)}$$

with $\sigma_{ij}^{(k)} = \int_{\mathbf{u}} u_i u_j g^{(k)}(\mathbf{u}) d\mathbf{u}$, in such a way that $\sigma^{(k)}$ is the related covariance matrix. Up to a rotation, the linear transformation $\mathbf{L}^{(k)}$, which is chosen as a Cholesky decomposition of $\sigma^{(k)}$ in the rotated set of axes, allows a natural change of variable. With this choice, we take $\mathbf{A} = (R^{(k)} \mathbf{L}^{(k)})^T$ and introduce the vector $\mathbf{X} = [X_1, X_2]$, defined by $\mathbf{X} = \mathbf{A}^{-1}(\mathbf{v} - \mathbf{U}_p)$, so that $\mathbf{v} = \mathbf{A}\mathbf{X} + \mathbf{U}_p$. This variable is a good candidate in order to perform tensorial one-dimensional quadrature based on the set of reconstructed centered third-order moments in the two new basis directions. There are fundamental grounds for using the Cholesky decomposition rather than the other methods. Defining the linear

transformation matrix \mathbf{A} in terms of the eigenvectors of the covariance matrix is a very good choice for the passive transport of a distribution function. However, because the velocity is a dynamic variable (i.e. the spatial fluxes are computed using the velocity abscissas through a kinetic scheme), the properties of the eigenvectors make them a poor choice for $d = 3$. The fundamental difficulty is the fact that the eigenvectors of $\sigma^{(k)}$ do not vary smoothly with its components. As a consequence, the fluxes computed from the abscissas are then discontinuous, leading to ‘random’ fluctuations in the moments. In contrast, the Cholesky matrix $\mathbf{L}^{(k)}$ with $\mathbf{R}^{(k)} = \text{Id}$, varies smoothly with the components of $\sigma^{(k)}$ and, hence, the fluxes are well-behaved [5].

On the other hand, the disadvantage of using the Cholesky matrix is that it depends on the ordering of the covariance matrix, and is thus different for each of the two permutations (six in three dimensions) of the coordinates corresponding to the two $\mathbf{R}^{(k)}$ matrices identity and rotation by $\pi/2$. It is thus desirable to replace $\mathbf{L}^{(k)}$ in any of the two preceding choices with a permutation-invariant linear transform. In order to do so, note that the transformation is not unique because of the presence of the $\mathbf{R}^{(k)}$ matrix. Here we use the two Cholesky decompositions $\mathbf{L}_{\mathbf{x}}^{(k)}$ and $\mathbf{L}_{\mathbf{y}}^{(k)}$ and consider the half angle between these two transformations. This transformation treats each direction the same manner, and is now independent of the ordering of the covariance matrix. Besides this choice is stable and defines a subspace of the moment space in which the conservative variables live.

3.3. Numerical methods

The transport in physical space obeys a system of weakly hyperbolic conservation laws and relies on kinetic finite volume schemes as introduced by [11] in order to solve the pressure-less gas dynamics equation. Once a quadrature method is designed, it defines a kinetic description that is equivalent to the moment system of equations for smooth solutions and allows to properly define the fluxes for transport of the moments in one space dimension. The resulting scheme is second-order accurate in space and time for the multi-fluid model, and first order in space and time for the multi-fluid multi-velocity model [5] in order to strictly preserve the moment space during the reconstruction part of the algorithm, that is to guarantee that the eigenvalues of the covariance matrix are both non-negative. In this contribution, we aim at working also at the boundary of the moment space since we want to tackle cases where the velocity distribution is reduced to a monokinetic distribution where the proposed quadrature degenerates to the original multi-fluid model and the covariance matrix can be zero up to machine precision.

Because of the transport in physical space and the transport in phase space through evaporation and drag have different structures, we use a Strang splitting algorithm [4,3]. The interest is two-fold. First, this approach has the great advantage of preserving the properties of the schemes we use for the different contributions, as, for example, maximum principle or positivity. If we assume that the phenomena involved evolve at roughly the same time scales, this Strang splitting algorithm guarantees second-order accuracy in time provided that each of the elementary schemes has second-order time accuracy. Furthermore, from a computational point of view, this is optimal and yields high parallelization capabilities. For the transport in physical space, we further use a dimensional Strang splitting of the 1D scheme previously described in [4]. The corresponding scheme offers the ability to treat the delta-shocks and vacuum states, and preserves the positivity of mass density as well as the moment space.

The preservation of the moment space is also important during transport in phase space. The local dynamical system defined in Eq. (1) or (2) can be rewritten $\partial_t Y^j = \Phi(Y^j)$, with, in case of the multi-fluid multi-velocity method,

$$Y^j = (m^j, m^j M_{10}^j, m^j M_{01}^j, m^j M_{20}^j, m^j M_{11}^j, m^j M_{02}^j, m^j M_{30}^j, m^j M_{21}^j, m^j M_{12}^j, m^j M_{03}^j)$$

This system is solved using an implicit Runge–Kutta Radau IIA method of order 5 with adaptive time steps. Whereas this resolution in case of multi-fluid method does not yield any difficulty, for the multi-velocity case it can lead to a non realizable set of Y^j . The preservation of the moment space requires working with the centered moments:

$$m^{(k)} \tilde{M}_{j,l}^{(k)} = \int_{S_{k-1}}^{S_k} \rho_l S^{3/2} \int_{\mathbf{u}} (u_x - M_{1,0}^{(k)})^j (u_y - M_{0,1}^{(k)})^l f(t, \mathbf{x}, S, \mathbf{u}) \, d\mathbf{u} \, dS$$

for $j + l \geq 2$. Starting from there, even if it leads to additional nonlinear terms in the ODE system, the Radau solver can be adapted and yields a robust solver on the conservative centered moments that strictly preserves the moment space and allows working up to the boundary of the moment space, i.e., the monokinetic velocity distribution.

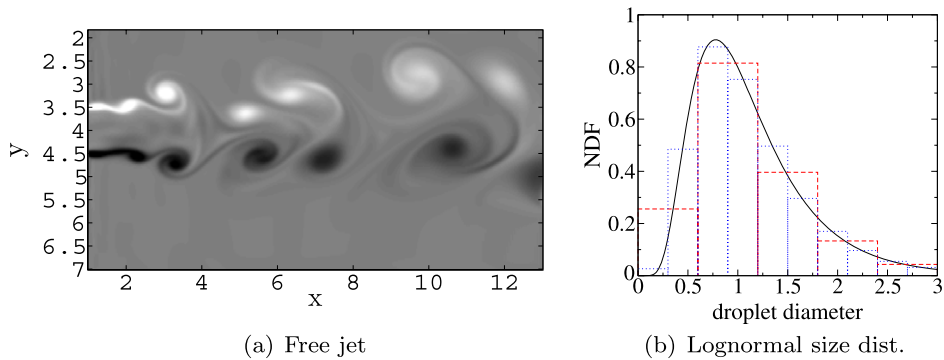


Fig. 3. Free jet configuration: (left) gaseous vorticity at time $t = 20$, obtained on a 400×200 grid; (right) polydisperse lognormal distribution discretized with 5 to 10 sections.

4. Free jet configuration and reference solutions

In order to assess the Eulerian methods we focus on a 2D Cartesian free jet. A polydisperse spray is injected in the jet core with a lognormal size distribution (Fig. 3-right), whose mean diameter d_0 corresponds to the reference surface S_0 . The simulations are conducted with a code that couples a gas solver to a Lagrangian solver (both developed at CORIA) and to a Eulerian solver (developed at EM2C) wherein the multi-fluid and multi-fluid multi-velocity methods are implemented.

As far as the gas phase is concerned, we used a 2D Cartesian low Mach number compressible solver. The gas jet is computed on a 400×200 grid. To destabilize the jet, we inject turbulence thanks to the Klein method with 10% fluctuations [12]. The Reynolds number based on U_0 , ν_0 and L_0 is 1000, where U_0 is the injection velocity and L_0 is the jet width. We will eventually provide dimensional quantities for illustration purposes. These will be based on an estimated velocity of $U_0 = 1$ m/s and $L_0 = 1.5 \times 10^{-2}$ m, as well as a typical value of 1.6×10^{-5} m²/s for ν_0 . Finally we have $d_0 = L_0/300$, where d_0 is the diameter corresponding to the typical droplet surface S_0 . The gas vorticity is presented in Fig. 3-left. Since we aim at validating the Eulerian models through comparisons to a Lagrangian simulation, and at providing an evaluation of the relative computational cost, we restrict ourselves to one-way coupling. We take as a reference solution for the liquid phase a Lagrangian Discrete Particle Simulation with 10,000 up to 70,000 particles in the computational domain depending on the cases. The number of droplets is determined by stoichiometry. We provide comparisons between this Lagrangian reference and the Eulerian multi-fluid and multi-fluid multi-velocity computations plotting the Lagrangian particle positions versus the Eulerian number density. Thanks to the multi-fluid polydispersion resolution, we perform the comparisons for different ranges of sizes and thus for various inertia, in the evaporating and non-evaporating cases.

4.1. Lagrangian vs. multi-fluid for evaporating and non-evaporating sprays

For the non-evaporating case we use five sections for the Eulerian multi-fluid simulation. We have 70,000 Lagrangian particles in the computational domain at the considered time. We present in this section a comparison for low inertia droplets and find a very good agreement for the droplets with a Stokes range from 0.011 to 0.12 corresponding to diameters from 9 μm to 30 μm , as shown in Fig. 4. The multi-fluid method is thus shown to simulate the dynamics of a polydisperse spray where droplet crossings are limited. Droplet dynamics are close to the gas dynamics for this range of sizes, and the model remains therefore in its validity domain (see Section 3.1). In fact, the same level of comparison is obtained for any of the five size ranges in the simulation as will be presented below for the evaporating case.

The free jet is also assessed with an evaporating spray. For the d^2 law, we take a constant mass transfer number $Bm = 0.1$. The results are presented the same way as for the non-evaporating case. In order to describe accurately the evaporation process, we take ten sections for the Eulerian multi-fluid simulation, whereas 30,000 Lagrangian particles are present in the domain at the considered time. As in the non-evaporating case, we found a very good agreement between the Eulerian multi-fluid and the Lagrangian descriptions. In this case, we focus on the size-conditioned dynamics of higher Stokes number droplets. These more inertial droplets are ejected from the vortices and crossing

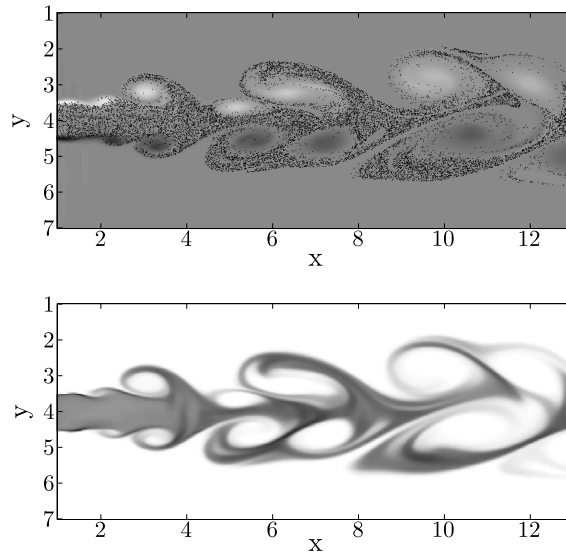


Fig. 4. Non-evaporating polydisperse spray, low inertia droplets, Stokes 0.011 to 0.12 corresponding to diameters $d = 9 \mu\text{m}$ to $d = 30 \mu\text{m}$, at time $t = 20$: (top) Lagrangian particle positions with 40,000 particles over gas vorticity, (bottom) Eulerian number density on a $400 \times 200 \times 5$ grid.

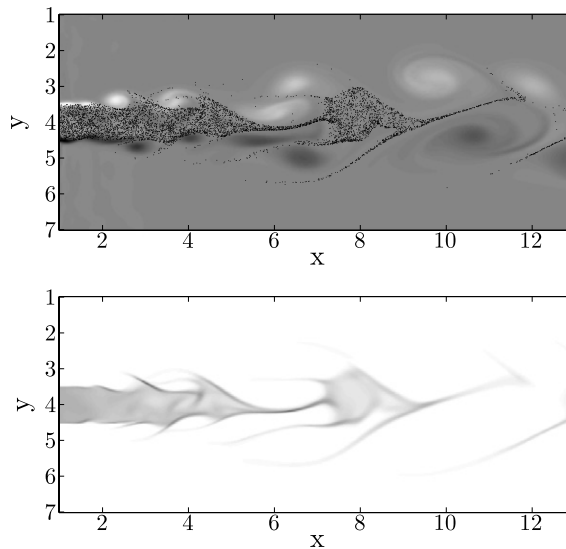


Fig. 5. Evaporating polydisperse spray, high inertia droplets, Stokes 0.48 to 1.1 corresponding to diameters $d = 60 \mu\text{m}$ to $d = 90 \mu\text{m}$, at time $t = 20$: (top) Lagrangian particle positions with 7000 particles over gas vorticity, (bottom) Eulerian number density with a $400 \times 200 \times 10$ grid.

trajectories are likely to occur, breaking the monokinetic multi-fluid assumption described in Section 3.1. Nevertheless, the dynamics are still very well reproduced for higher Stokes numbers. The results are plotted in Fig. 5 for Stokes numbers from 0.48 to 1.1 corresponding to diameters from $60 \mu\text{m}$ to $90 \mu\text{m}$. One can notice that the number density is concentrated in a few cells in this case and the numerical method does not encounter any problem to capture it, illustrating again the method's robustness and accuracy.

This polydisperse evaporating free jet shows the ability of the multi-fluid method to treat more complex cases, closer to realistic configurations. From these comparisons, we demonstrate that the Eulerian method captures size-conditioned dynamics that carry droplets of different size to different locations. It is then essential to evaluate the ability of the Eulerian model to capture the evaporation process as a whole.

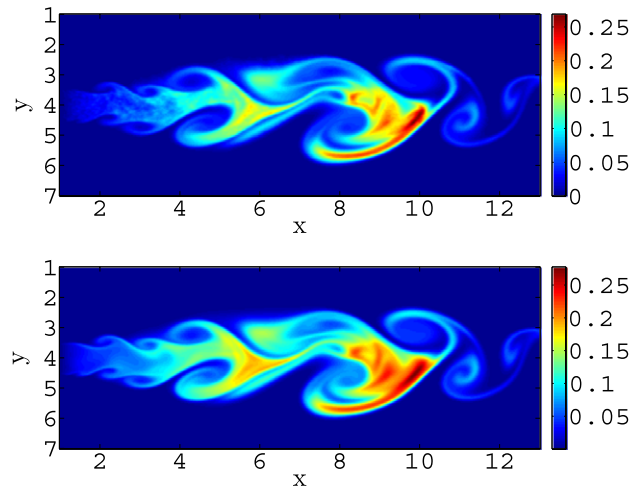


Fig. 6. Comparison of the gaseous fuel mass fraction at time $t = 20$, obtained from evaporation using (top) a Lagrangian method with 30,000 droplets at the considered time and (bottom) a Eulerian multi-fluid model with a $400 \times 200 \times 10$ mesh.

Our interest being in combustion applications, a key issue of evaporating spray modeling is the gaseous fuel mass fraction prediction. We thus present comparisons between this gaseous fuel mass fraction, obtained from the Lagrangian and the Eulerian multi-fluid descriptions of the spray. These results are obtained within the same coupled code run, the spray being described on the one hand by the Lagrangian method and on the other hand by the Eulerian multi-fluid model. This simulation is still done using a one-way coupling. Indeed, the evaporated fuel is not added as a mass source term in the gaseous equations, but is stored in two passive scalars, one for each description of the spray, that are transported by the flow. The Lagrangian gaseous fuel mass fraction is obtained through a projection of the droplet evaporation over the neighbor cells of the gaseous mesh. These two fields are plotted in Fig. 6. One can see the very good agreement of both descriptions for spray evaporation. This comparison underlines the efficiency of the Eulerian multi-fluid model in describing polydisperse evaporating sprays. Furthermore, as we can see in Fig. 6, the Eulerian description provides a smoother field than the Lagrangian one. It illustrates the difficulties arising when coupling the Lagrangian description of the liquid to the Eulerian description of gas and underlines the advantage of the Eulerian description of the spray for the liquid–gas coupling. These results are a first step towards combustion computations.

4.2. Multi-fluid multi-velocity model versus Lagrangian method

For the simulations with multi-velocity model, the first step is to show the good level of agreement between the Eulerian model and the Lagrangian simulation. Thus, Fig. 7-left presents a fair comparison, similar to the level obtained in previous simulations. In order to quantify the ability of the method to capture droplet crossing, we have also plotted in the right part of the figure the half trace of the covariance matrix, which amount to a “temperature” in the case of isotropic velocity distributions. However, since this is also present in areas of very small mass due to numerical diffusion, we have also plotted the absolute value of the difference of the two eigenvalues of this matrix, thus showing areas where there is strong anisotropy and corresponding to crossing “in progress”. This very beautifully fits with the plots in Fig. 7-left.

Finally, we have plotted the results of the multi-velocity model with evaporation in the case of the polydisperse spray jet in Fig. 8. Once again, this figure demonstrates the ability of the proposed method to capture the dynamics conditioned by size as well as evaporation for a range of small to finite Stokes numbers.

5. Conclusions

In this paper, we have described a new multi-fluid multi-velocity Eulerian model that is able to capture both polydispersity and size-conditioned dynamics, and droplet crossings for evaporating sprays. Using this model, we

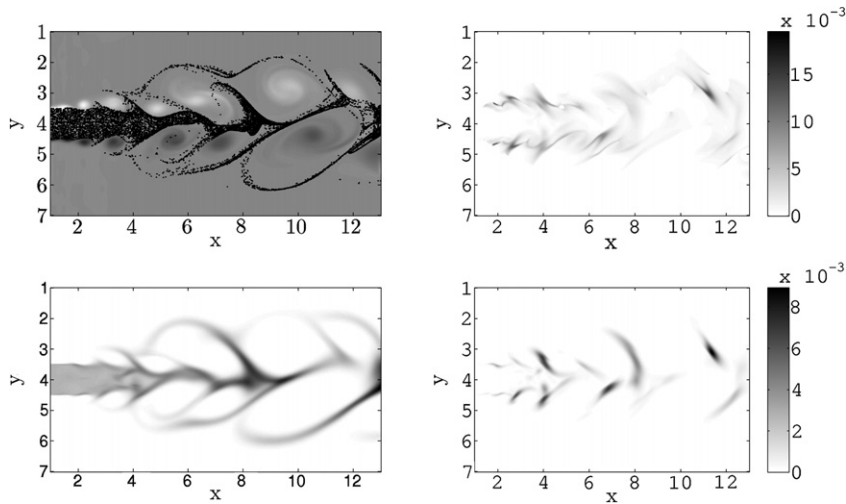


Fig. 7. Non-evaporating polydisperse spray, high inertia droplets, Stokes 0.48 to 1.1 corresponding to diameters $d = 60 \mu\text{m}$ to $d = 90 \mu\text{m}$, at time $t = 20$: (top-left) Lagrangian particle positions with 20,000 particles over gas vorticity, (bottom-left) Eulerian number density with a $400 \times 200 \times 5$ grid. Evaluation of the trace of the covariance matrix (right-top) as well as the absolute value of the difference between the two eigenvalues highlighting the zones of droplet crossing (right-bottom).

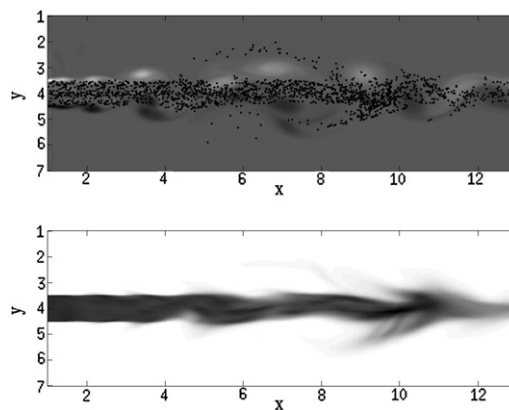


Fig. 8. Evaporating polydisperse spray, high inertia droplets, Stokes 0.48 to 1.1 corresponding to diameters $d = 60 \mu\text{m}$ to $d = 90 \mu\text{m}$, at time $t = 15$: (top) Lagrangian particle positions with 7000 particles over gas vorticity, (bottom) Eulerian number density with a $400 \times 200 \times 10$ grid.

have conducted a series of detailed comparisons with a Lagrangian solver in the configuration of a 2D free jet, and shown the capability of the Eulerian model to reproduce very accurately the Lagrangian results, from small Stokes numbers up to finite Stokes of order one, where droplet crossings become important. We thus claim that we have validated the proposed model.

However, one important issue that has yet to be addressed is the relative computational cost. The DPS conducted here is roughly 10 times faster than the corresponding Eulerian multi-fluid model simulated sequentially. It corresponds to a single realization of the Williams equation, and can be shown to contain information much noisier than the Eulerian model with the given discretization. In a complementary study, we have investigated, in different configurations, this issue and shown that a real DSMC resolution of the Williams equation associated to a same level of refinement of the Eulerian fields leads to a similar cost between the two approaches [4,13]. Thus, this is promising for the Eulerian model since it has also been shown to have a high parallelization capability and scalability for 3D calculations in [14].

Acknowledgements

This research was supported by an ANR-05-JC05_42236 Young Investigator Award (M. Massot), by a DGA/CNRS Ph.D. grant for S. de Chaisemartin and through a PEPS CNRS project (ST2I and MPPU – F. Laurent). Part of this work was performed during the 2008 Summer Program at the Center for Turbulence Research with financial support from Stanford University and NASA Ames Research Center.

References

- [1] F.A. Williams, Spray combustion and atomization, *Physics of Fluids* 1 (1958) 541–545.
- [2] G.A. Bird, *Molecular Gas Dynamics and the Direct Simulation of Gas Flows*, Oxford Science Publications, vol. 42, 1994.
- [3] M. Massot, Eulerian multi-fluid models for polydisperse evaporating sprays, in: D.L. Marchisio, R.O. Fox (Eds.), *Multi-Phase Reacting Flows: Modelling and Simulation*, in: CISM Courses and Lectures, vol. 492, Springer, Wien, 2007, chapter III, pp. 79–123.
- [4] S. de Chaisemartin, F. Laurent, M. Massot, J. Reveillon, Evaluation of Eulerian multi-fluid versus Lagrangian methods for the ejection of polydisperse evaporating sprays by vortices, *Journal of Computational Physics* (2009), submitted for publication, available on HAL, <http://hal.archives-ouvertes.fr/hal-00169721/>.
- [5] R.O. Fox, A quadrature-based third-order moment method for dilute gas-particle flow, *Journal of Computational Physics* 227 (12) (2008) 6313–6350.
- [6] J. Reveillon, C. Péra, M. Massot, R. Knikker, Eulerian analysis of the dispersion of evaporating polydispersed sprays in a statistically stationary turbulent flow, *Journal of Turbulence* 5 (1) (2004) 1–27.
- [7] L. Freret, S. de Chaisemartin, F. Laurent, P. Vedula, R.O. Fox, O. Thomine, J. Reveillon, M. Massot, Eulerian moment models for polydisperse weakly collisional sprays: model and validation, in: *Proceedings of the Summer Program 2008*, Center for Turbulence Research, Stanford University, 2009.
- [8] F. Laurent, M. Massot, Multi-fluid modeling of laminar poly-dispersed spray flames: origin, assumptions and comparison of sectional and sampling methods, *Combustion Theory and Modelling* 5 (2001) 537–572.
- [9] J.B. Greenberg, I. Silverman, Y. Tambour, On the origin of spray sectional conservation equations, *Combustion and Flame* 93 (1993) 90–96.
- [10] M. Massot, F. Laurent, D. Kah, S. de Chaisemartin, A robust moment method for evaluation of the disappearance rate of evaporating sprays, *SIAM J. Appl. Math.* (2009), submitted for publication, available on HAL, <http://hal.archives-ouvertes.fr/hal-00332423/fr/>.
- [11] F. Bouchut, S. Jin, X. Li, Numerical approximations of pressureless and isothermal gas dynamics, *SIAM Journal on Numerical Analysis* 41 (2003) 135–158.
- [12] M. Klein, A. Sadiki, J. Janicka, A digital filter based generation of inflow data for spatially developing direct numerical or large eddy simulations, *Journal of Computational Physics* 186 (2003) 652–665.
- [13] S. de Chaisemartin, F. Laurent, M. Massot, J. Reveillon, Complete report with comparisons of Lagrangian and Eulerian formulation from both the physical and the numerical point of view, Technical report, CRSA-EM2C, Deliverable 1.3.1b, European Project TIMECOP-AE, 2006.
- [14] S. de Chaisemartin, Modèles Eulériens et simulation de la dispersion turbulente de brouillards qui s'évaporent, Ph.D. thesis, Ecole Centrale Paris, 2009.